XLIII CILAMCE
21–25, November, 2022
FOZ DO IGUAÇU – PR – BRAZIL

Solution construction for a drainage process for a system modeling the foam flow with linear surfactant adsorption

Giulia C. Fritis[1], Pavel Z. S. Paz[1], Grigori Chapiro[1]

[1]*Laboratory of Applied Mathematics (LAMAP), Federal University of Juiz de Fora. José Lourenço Kelmer - São Pedro, Juiz de Fora, 36036-900, Minas Gerais, Brazil*
giufritis@gmail.com, pavel.sejas.paz@ice.ufjf.br, grigori@ice.ufjf.br

Abstract.

In this work, we present an analytical solution for a drainage process of a system of non-strictly hyperbolic Conservation Laws describing the foam flow in porous media under effect of linear adsorption of surfactant. We adopt a system composed of two differential equations, one modeling the conservation of saturation of the wetting phase and the other the conservation of chemical in the wetting phase with linear surfactant adsorption.

The foam flow dynamic is assumed to follow the implicit texture STARS model. In this model, the foam texture assumes local equilibrium, meaning that the foam formation rapidly attains a state where the bubbles generation rate matches the coalescence rate. We present a geometrical construction of the analytical solution and compare our results with a direct numerical simulation.

Keywords: Foam flow, Surfactant flooding, STARS model, Linear adsorption, EOR

1 Introduction

The use of foam in porous media has gained interest in the scientific community due to various applications, including in the petroleum industry and the recovery of contaminated soil Zavala et al. [1]. Despite its high efficiency, gas injection for enhanced oil recovery (EOR) is susceptible to reduction because of gravitational gradients, reservoir heterogeneity, and other instabilities. All these issues with gas sweeping can be mitigated using foam Ashoori et al. [2]. Appropriate use of foam can result in a significant reduction in the gas phase mobility, leading to a better sweeping of porous media Kam [3].

Surfactant reduces the surface tension and capillary effects, enabling the formation of bubbles. The surfactant molecules are susceptible to adsorbing on rock surfaces, affecting the surfactant concentration, which can lead to foam destabilization Cantat et al. [4]. The high costs of chemicals and their loss due to adsorption can make such a process economically unfeasible.

We use a Conservation Laws system that describes the foam flow and the transport of surfactants in the wetting phase with their adsorption on porous media surfaces. This system is formed by two phases: a wetting phase, composed of the mixture of water and surfactant, and a gaseous phase, where foam is a tracer. We adopted the fractional flow function implemented in one of the industry simulators most used for EOR, the CMG simulator with STARS model Cantañeda et al. [5]. This model assumes local equilibrium, which means that the foam formation is attained immediately and is represented implicitly in the model by a mobility reduction factor of the gas permeability depending on water saturation and surfactant concentration.

This work is organized as follows: In Section 2 we present and describe governing equations that model this problem. In Section 3 we briefly present the main concepts about the waves involved in the solution. In Section 4 we construct the analytical solution using a geometric representation. Finally, in Subsection 4.1 we present a comparison between the analytical solution and a numerical approach performed by the Reaction Convection Diffusion Equations Solver (RCD).

2 Mathematical model

To describe the foam and chemical transport with linear surfactant adsorption on porous media surfaces, we adopt the following system

$$\partial_t S + \partial_x f(S, C) = 0, \tag{1}$$

$$\partial_t \left[(S + \mathcal{A})C\right] + \partial_x \left[f(S, C)C\right] = 0, \tag{2}$$

where S and C are the dimensionless and normalized saturation of the aqueous phase and surfactant concentration respectively, $(S, C) \in I \times I$ with $I = [0, 1]$, $(x, t) \in \mathbb{R} \times \mathbb{R}^+$, $f : I \times I \to \mathbb{R}$ is the fractional flow function of the aqueous phase and $\mathcal{A}$ is a constant that represents the linear adsorption of the surfactant in rock surfaces. A similar system was presented in the work of Isaacson [6], where he considered the oil displacement by polymer flooding, but the chemical adsorption was neglected. Our approach is different from the one of Isaacson; while he considered an increase of water viscosity by the presence of polymer, our model represents the foam formation through a mobility reduction factor of the gas relative permeability.

To use Buckley and Leverett [7] fractional flow theory, we assume: 1D horizontal flow, Newtonian mobilities, absence of capillary pressure gradient, negligible gravitational effects, no dispersion, incompressible phases, no viscous "fingering", and immediate reach to the local steady-state.

The superficial velocity of the j phase, with $j =$\{water, gas\}, is given by

$$u_w = -\frac{k k_{rw}}{\mu_w}\nabla p, \quad u_g = -\frac{k k_{rg}^f}{\mu_g}\nabla p, \tag{3}$$

where k is the permeability of the porous medium, μ_j is the viscosity of the phase j, ∇p is the pressure gradient, and k_{rj} are the relative permeabilities of the phase j, which can be expressed by

$$k_{rj} = k_{rj}^0 \left(\frac{S_j - S_{jr}}{1 - S_{wc} - S_{gr}}\right)^{n_j}, \tag{4}$$

where k_{rj}^0 is the end point relative permeability of the phase j, n_j is Corey's exponent, S_j is the saturation of the phase j, and S_{wc} and S_{gr} are the connate water saturation and residual gas, respectively.

The term k_{rg}^f in eq. (3) represents the relative permeability of the gas phase in the presence of foam, which can be expressed by

$$k_{rg}^f = k_{rg} \cdot FM, \tag{5}$$

where FM is the mobility reduction factor following the STARS model Zeng et al. [8], which is defined as

$$FM = \frac{1}{1 + fmmob \cdot F_1(C_s) \cdot F_2(S_w)}, \tag{6}$$

where $fmmob$ represents the reference mobility reduction factor, and C_s is the surfactant concentration.

The function F_2 describes the water saturation effects and is given by

$$F_2(S_w) = \frac{1}{2} + \frac{\arctan(epdry \cdot (S_w - fmdry))}{\pi}, \tag{7}$$

where $fmdry$ is the critical water saturation, and $epdry$ represents the abruptness of the dry-out effects. F_1 function introduces the surfactant concentration effects, defined as

$$F_1(C_s) = \begin{cases} \left(\dfrac{C_s}{fmsurf}\right)^{epsurf}, & \text{If } C_s < fmsurf, \\ 1, & \text{If } C_s \geq fmsurf, \end{cases} \tag{8}$$

where $fmsurf$ is the critical surfactant concentration and $epsurf$ is an exponent parameter.

The fractional flow function of the aqueous phase is defined as $f = u_w/u$, where $u = u_w + u_g$ is the total superficial velocity.

Let us consider the dimensionless temporal and spatial variables as follows

$$t' = \frac{u}{(1 - S_{wc} - S_{gr})\phi L}t, \quad x' = \frac{x}{L}, \tag{9}$$

where L is the 1D length of the reservoir and ϕ is the porous media porosity. The system of eqs. (1)-(2) is presented with the dimensionless variables dropping out the prime symbol. The dimensionless and normalized water saturation and surfactant concentration adopted here are

$$S = \frac{S_w - S_{wc}}{1 - S_{wc} - S_{gr}}, \quad C = \frac{C_s^w}{C_{\max}}, \tag{10}$$

where $C_{\max}$ is the maximum surfactant concentration.

The constant $\mathcal{A}$ is given by

$$\mathcal{A} = \frac{1}{1 - S_{wc} - S_{gr}} \left(S_{wc} + \frac{(1-\phi)\rho_s K_d^a}{\rho_w \phi} \right), \tag{11}$$

where ρ_w and ρ_s are the water and rock density, respectively. K_d^a is the proportionality constant between the surfactant concentration adsorbed on rock surfaces and the surfactant concentration injected.

We aim to present a solution for the drainage process, which we describe as a Riemann problem. In this way, we want to obtain a solution for the system of eqs. (1)-(2) associated with the initial data in the form

$$(S(x,0), C(x,0)) = \begin{cases} (S_J, C_J), & \text{if } x < 0, \\ (S_I, C_I), & \text{if } x \geq 0, \end{cases} \tag{12}$$

where the subscripts J and I represent the injection and initial condition, respectively. We emphasize that the system of eqs. (1)-(2) with C is constant reduces to a typical Buckley-Leverett solution.

3 Study of the Riemann problem

The system of eqs. (1)-(2) can be rewritten in the conservative form as

$$\partial_t U + A(U)\partial_x U = 0, \tag{13}$$

where U denotes the state $U = (S, C)^T$ and $A(U)$ is a 2×2 upper triangular matrix, given by

$$A(U) = \begin{pmatrix} \partial_S f & \partial_C f \\ 0 & f/(S + \mathcal{A}) \end{pmatrix}. \tag{14}$$

The eigenvalues and eigenvectors associated with the matrix A are

$$\lambda_C = f/(S+\mathcal{A}), \quad r_C = \left(\partial_C f, f/(S+\mathcal{A}) - \partial_S f\right)^T, \tag{15}$$

$$\lambda_S = \partial_S f, \qquad r_S = (1,0)^T. \tag{16}$$

For each fixed C, there is a unique $S^* = S^*(C) \in I$ such that

$$\lambda_S(S^*, C) = \lambda_C(S^*, C). \tag{17}$$

Geometrically, the points satisfying eq. (17) are those that the secant line connecting them and $(-\mathcal{A}, 0)$ possesses the same slope as the tangent of f at this point. The set of points that satisfy eq. (17) defines a curve called **transition curve** and is denoted by $\mathcal{T}$. We remark that in this set our system of eqs. (1)-(2) is not strictly hyperbolic.

Following the Conservation Laws Theory, see Smoller [9], the C characteristic family satisfies $\nabla\lambda_C \cdot r_C = 0$, and therefore is linearly degenerate. The solutions in linearly degenerate characteristic families are called contact discontinuities. A contact discontinuity connecting the state U_L to the state U_R with velocity γ satisfies the generalized Lax's entropy condition if

$$\lambda_S(U_L) \leq \gamma,\ \lambda_S(U_R) \leq \gamma \quad \text{or} \quad \lambda_S(U_L) \geq \gamma,\ \lambda_S(U_R) \geq \gamma. \tag{18}$$

Once the contact velocity is given by $\gamma = \lambda_C(U_L) = \lambda_C(U_R)$, we conclude that the contact discontinuity satisfies this entropy condition when connecting states on the same side of $\mathcal{T}$. We denote the solutions in the C characteristic family by C-waves.

The S characteristic family is not degenerated and possesses solutions in the form of shock waves, rarefaction waves, or a combination of both. If a shock connects the states U_L and U_R, respectively, its velocity satisfies the Rankine-Hugoniot (RH) condition, given by

$$s = \frac{f(U_R) - f(U_L)}{S_R - S_L}, \tag{19}$$

where s is the shock propagation velocity. On the other hand, when a rarefaction wave connects U_L and U_R, its initial velocity is given by $\lambda_S(U_L)$ and its final velocity is defined as $\lambda_S(U_R)$.

Due to the properties of the shock and rarefaction waves, together with the generalized Lax's entropy condition (see Leveque [10] for more details), these waves keep C constant and follow the Buckley-Leverett solution. We refer to these solutions as S-waves.

4 Solution for a Riemann problem for drainage

In this section, we present a geometric construction of the analytical solution for the system of eqs. (1)-(2) for a drainage case. For this purpose, we use the data from Valdez et al. [11], which are listed in Table 1. The geometric construction presented here is similar to the one made by Dindoruk and Dindoruk [12].

The drainage process is defined as the injection of the non-wetting phase, aiming to recover the wetting phase. For a two-phase system composed of water with surfactant and gas, this process injects gas into the porous media saturated with the wetting phase, thus forming bubbles.

For the example presented in Fig. 1, we set $U_L = (0.2, 0)$ and $U_R = (0.9, 0.5)$ as injection and initial conditions, respectively. However, the procedure is valid for any drainage condition in which the flux curve f possesses S-shape. As previously commented, the S-waves keep the value of C constant, implying that the value of C only changes through a C-wave.

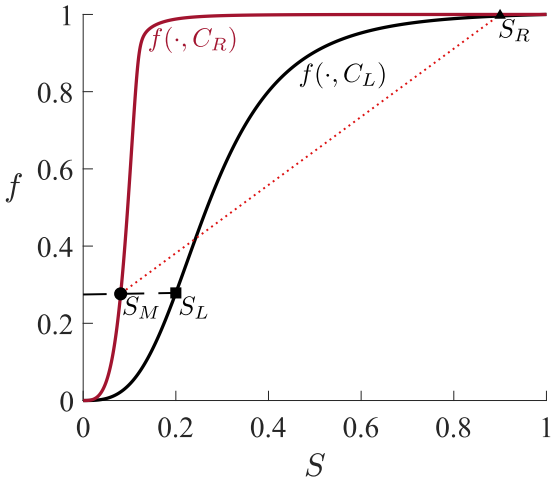

Figure 1. The Figure shows the left state (solid black line) and the right state fractional flow function (red solid line). The secant line from $(-\mathcal{A}, 0)$ to $(S_L, f(U_L))$ (black traced line) and the secant line from $(S_M, f(U_M))$ to $(S_R, f(U_R))$ (red dotted line). The injection stars in $U_L = (0.2, 0)$ and ends in $U_R = (0.9, 0.5)$, with the intermediate state $U_M = (0.0809, 0.5)$.

Our solution construction is composed of a C-wave from U_L to U_M, followed by a S-wave from U_M to U_R. The intermediate state U_M is connected to U_L by a contact discontinuity, with velocity

$$\lambda_C(U_L) = \frac{f(U_L)}{S_L + \mathcal{A}} = \frac{f(U_M)}{S_M + \mathcal{A}} = \lambda_C(U_M). \tag{20}$$

Geometrically, this velocity is the slope of the secant line that connects $(S_L, f(U_L))$, $(S_R, f(U_R))$ and $(-\mathcal{A}, 0)$. Thus, the intermediate state U_M is defined as the intersection of the secant line connecting $(-\mathcal{A}, 0)$ and $(S_L, f(U_L))$ with the function $f(\cdot, C_R)$. This intersection happens at least in one point, once $f(\cdot, C_L) \leq f(\cdot, C_R)$. In the case of more than one intersection, the generalized Lax's entropy condition establish which state we must take as U_M.

The second wave that composes our solution is an S-wave, which keeps C fixed. Accordingly, the states U_M and U_R possess the same fractional flow function. Then, by Oleinik's entropy condition Leveque [10], we conclude that a shock wave occurs between U_M and U_R.

We must verify the wave compatibility, i.e., whether the wave velocities remain the same or increase. Once our solution is composed of a contact discontinuity followed by a shock wave, we must confirm if the contact velocity is less or equal to the shock velocity. The shock velocity that connects the states U_M to U_R is given by

$$s = \frac{f(U_R) - f(U_M)}{S_R - S_M}. \tag{21}$$

Geometrically, this velocity is the slope of the secant line through $(S_M, f(U_M))$ and $(S_R, f(U_R))$. As previously commented, the contact velocity is the slope of the secant that connects $(S_L, f(U_L))$ and $(-\mathcal{A}, 0)$. To conclude that the wave sequence is compatible, it is necessary to compare the slope of those secant lines.

The geometrical construction explained above is presented in Fig. 1. It is shown that the secant line connecting $(-\mathcal{A}, 0)$ to $(S_L, F(U_L))$ (black traced line) has smaller slope than the secant line connecting $(S_M, f(U_M))$ and $(S_R, f(U_R))$ (red pointed line). Therefore, we conclude that the wave sequence is compatible.

4.1 Comparison of analytical solution with numerical approach

To obtain a numerical solution for the system of eqs. (1)-(2) with initial data in the form of eq. (12), we use the RCD solver Lambert et al. [13]. This solver is based on the finite differences scheme, Crank-Nicolson, combined with Newton's method and has second-order accuracy in space and time. The boundary condition on the left was Dirichlet and Neumann on the right. For the spatial discretization, we used 8000 points; for the time discretization, the time step adopted was 10^{-5}. No artificial diffusion was added to the system.

Figure 2 presents a comparison between the analytical solution obtained in Section 4 and the numerical solution performed by RCD. For this purpose, we use the injection condition $U_L = (0.2, 0)$ and the initial condition $U_R = (0.9, 0.5)$ for a dimensionless time $t = 0.8$. As one can observe both solutions are in excellent agreement with each other.

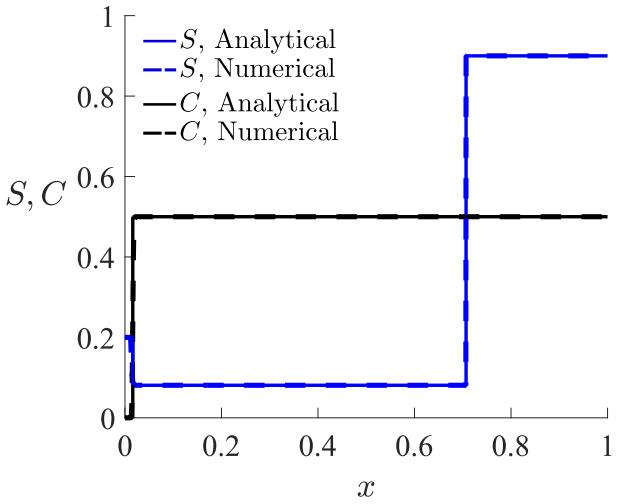

Figure 2. The Figure shows the comparison between the analytical solution (solid lines) an numerical approach (traced lines) with $U_L = (0.2, 0)$ and $U_R = (0.9, 0.5)$ for dimensionless time $t = 0.8$. The profiles in blue represent the water saturation and in black the surfactant concentration.

5 Conclusions

In this work, we consider a system of conversation laws that models the transport of mass water and surfactant in the wetting phase in a porous media containing gas and water. We assume the chemical linear adsorption of surfactant on rock surfaces. Also, we assume that the foam formation follows the local equilibrium STARS model implemented in the commercial simulator CMG. We establish our dimensionless Riemann problem and construct a compatible analytical solution involving fundamental waves (i.e., contact and shock waves) for a specific drainage process. In addition, we compared our analytical solution with the numerical solver RCD, obtaining excellent agreement between both solutions. The future scope of this work would include the complete solution to the Riemann problem.

Acknowledgements. The current work was conducted in association with the R&D projects ANP n° 20715-9, "Modelagem matemática e computacional de injeção de espuma usada em recuperação avançada de petróleo" (UFJF/Shell Brazil/ANP). Shell Brazil funds it in accordance with ANP's R&D regulations under the Research, Development, and Innovation Investment Commitment. This project is carried out in partnership with Petrobras.

Table 1. The parameters and values used to provide numerical comparison following Valdez et al. [11].

Symbol	Parameter	Value
k_{rw}^0	End-point water relative permeability	0.302
k_{rg}^0	End-point gas relative permeability	0.004
n_w	Corey's exponent for water	2.98
n_g	Corey's exponent for gas	0.96
μ_w	Water viscosity	1e-03 [Pa · s]
μ_g	Gas viscosity	5e-04 [Pa · s]
ϕ	Porosity	0.21
ρ_w	Water density	1000
ρ_s	Solid density	2000
$fmmob$	Mobility reduction factor	293.27
$fmdry$	Critical water saturation	0.437
$epdry$	Abruptness of dry out effect	359.33
S_{wc}	Water connate saturation	0.4
S_{gr}	Gas residual saturation	0.293
$fmsurf$	Critical surfactant concentration	2 [g/L]
$epsurf$	Exponent that controls the stiffness of foam strength	1 [g/L]
C_{max}	Maximum surfactant concentration	3
K_d^a	Adsorption constant	0.5
u	Velocity	2.5e-05 [m/s]
L	Length of the porous media	0.17 [m]

G. Chapiro was supported in part by CNPq grants 303245/2019-0 and 405366/2021-3, and FAPEMIG grant APQ-00405-21.

Authorship statement. The authors hereby confirm that they are the sole liable persons responsible for the authorship of this work, and that all material that has been herein included as part of the present paper is either the property (and authorship) of the authors, or has the permission of the owners to be included here.

References

[1] R. Q. Zavala, L. F. Lozano, P. L. Zitha, and G. Chapiro. *Analytical Solution for the Population-Balance Model Describing Foam Displacement*. Springer, 2021.

[2] E. Ashoori, D. Marchesin, and W. Rossen. Stability analysis of uniform equilibrium foam states for eor processes. *Transport in porous media*, vol. 92, n. 3, pp. 573–595, 2012.

[3] S. I. Kam. Improved mechanistic foam simulation with foam catastrophe theory. *Colloids and Surfaces A: Physicochemical and Engineering Aspects*, vol. 318, n. 1-3, pp. 62–77, 2008.

[4] I. Cantat, S. Cohen-Addad, F. Elias, F. Graner, R. Höhler, O. Pitois, F. Rouyer, and A. Saint-Jalmes. *Foams: structure and dynamics*. OUP Oxford, 2013.

[5] J. Tang, P. Castañeda, D. Marchesin, and W. R. Rossen. Three-phase fractional-flow theory of foam-oil displacement in porous media with multiple steady states. *Water Resources Research*, vol. 55, n. 12, pp. 10319–10339, 2019.

[6] E. Isaacson. *Global solution of a Riemann problem for a non-strictly hyperbolic system of conservation laws arising in enhanced oil recovery*, preprint.

[7] S. E. Buckley and M. Leverett. Mechanism of fluid displacement in sands. *Transactions of the AIME*, vol. 146, n. 01, pp. 107–116, 1942.

[8] Y. Zeng, K. Ma, R. Farajzadeh, M. Puerto, S. L. Biswal, and G. J. Hirasaki. Effect of surfactant partitioning between gaseous phase and aqueous phase on CO_2 foam transport for enhanced oil recovery. *Transport in Porous Media*, vol. 114, n. 3, pp. 777–793, 2016.

[9] J. Smoller. *Shock waves and reaction—diffusion equations*, volume 258. Springer Science & Business Media, 2012.

[10] R. J. LeVeque. *Numerical methods for conservation laws*, volume 214. Springer, 1992.

[11] A. R. Valdez, B. M. Rocha, da J. M. Fonseca Façanha, de A. V. O. Souza, A. Perez-Gramatges, G. Chapiro, and R. W. d. Santos. *Foam-Assisted Water–Gas Flow Parameters: From Core-Flood Experiment to Uncertainty Quantification and Sensitivity Analysis*. Springer, 2021.

[12] D. M. Dindoruk and B. Dindoruk. Analytical solution of nonisothermal buckley-leverett flow including tracers. *SPE Reservoir Evaluation & Engineering*, vol. 11, n. 03, pp. 555–564, 2008.

[13] W. Lambert, A. Alvarez, I. Ledoino, D. Tadeu, D. Marchesin, and J. Bruining. Mathematics and numerics for balance partial differential-algebraic equations (PDAES). *Journal of Scientific Computing*, vol. 84, n. 2, pp. 1–56, 2020.